



HAL
open science

OPTICAL FEEDBACK INTERFEROMETRY: FROM BASICS TO APPLICATIONS OF LASER FLOWMETRY

E Ramírez-Miquet, Julien Perchoux, Raul da Costa Moreira, Y. Zhao,
Antonio Luna Arriaga, Clément Tronche, O. Sotolongo-Costa

► **To cite this version:**

E Ramírez-Miquet, Julien Perchoux, Raul da Costa Moreira, Y. Zhao, Antonio Luna Arriaga, et al..
OPTICAL FEEDBACK INTERFEROMETRY: FROM BASICS TO APPLICATIONS OF LASER
FLOWMETRY . Revista Cubana de Fisica, 2017, 34 (1), pp.48 - 57. hal-01611682

HAL Id: hal-01611682

<https://laas.hal.science/hal-01611682>

Submitted on 6 Oct 2017

HAL is a multi-disciplinary open access archive for the deposit and dissemination of scientific research documents, whether they are published or not. The documents may come from teaching and research institutions in France or abroad, or from public or private research centers.

L'archive ouverte pluridisciplinaire **HAL**, est destinée au dépôt et à la diffusion de documents scientifiques de niveau recherche, publiés ou non, émanant des établissements d'enseignement et de recherche français ou étrangers, des laboratoires publics ou privés.

OPTICAL FEEDBACK INTERFEROMETRY: FROM BASICS TO APPLICATIONS OF LASER FLOWMETRY

INTERFEROMETRÍA DE RETROINYECCIÓN ÓPTICA: DESDE LOS FUNDAMENTOS HASTA LAS APLICACIONES DE LA FLUJOMETRÍA LÁSER

E. E. RAMÍREZ-MIQUET^{abc†}, J. PERCHOUX^{a†}, R. DA COSTA MOREIRA^a, Y. ZHAO^a, A. LUNA-ARRIAGA^a, C. TRONCHE^a AND O. SOTOLONGO-COSTA^d

a) LAAS-CNRS, Université de Toulouse, CNRS, INP, Toulouse F-31000, France; julien.perchoux@laas.fr[†]

b) Centro de Aplicaciones Tecnológicas y Desarrollo Nuclear. Calle 30, No. 502, Miramar C.P. 11300, La Habana, Cuba

c) On leave from a) and b). Currently at Laboratoire Matériaux et Phénomènes Quantiques, Université Paris Diderot, CNRS, Sorbonne Paris Cité, UMR 7162, 10 rue Alice Domon et Léonie Duquet, Paris 75013, France; eramirez@univ-paris-diderot.fr[†]

d) IICBA, CInC, Universidad Autónoma del Estado de Morelos, Avenida Universidad 1001, Cuernavaca, CP 62209 Morelos, Mexico

† corresponding author

Recibido 20/4/2017; Aceptado 18/5/2017

Optical feedback interferometry (OFI) is a contactless technique that is employed for measuring parameters related to object's motion. The light emitted by a laser is backreflected or scattered from a moving object and a small portion of the scattered waves re-enters the laser cavity and impacts the laser's emission properties. We review the theoretical basics of optical feedback interferometry and explain the physical principles in the frame of laser Doppler flowmetry. We present a model derived from the Lang and Kobayashi rate equations to show the particular features of the optical feedback signal in temporal and frequency domain. In addition, we present experimental measurements relative to the detection of flowing particles in a microchannel, the measurement of unsteady flows and the quantification of blood perfusion in skin, which demonstrate the potential use of OFI sensors in the assessment of fluidic systems of interest in chemical and biomedical engineering.

La interferometría de retroinyección óptica (IRO) constituye una técnica de no contacto utilizada para la medición de parámetros del movimiento. La luz emitida por un láser es esparcida por un objeto en movimiento y una pequeña parte de las ondas producto de esa dispersión entran en la cavidad del láser, impactando sus propiedades espectrales. Se presenta una revisión de las bases teóricas del efecto de la retroinyección óptica y se exponen sus principios físicos en el marco de la flujometría. Se presenta un modelo derivado de las ecuaciones de Lang y Kobayashi para mostrar las características principales de la señal de retroinyección óptica en dominio temporal y frecuencial. Adicionalmente, se presentan resultados experimentales relativos a la medición de partículas fluyendo dentro de un microcanal, la medición de flujos no estacionarios y la cuantificación de la perfusión sanguínea en la piel, los cuales demuestran los usos potenciales de los sensores IRO para el análisis de sistemas fluidicos de interés para la ingeniería química y biomédica.

PACS: Optical feedback interferometry, microfluidic device, particle detection, non-steady flows, blood perfusion.

I. INTRODUCTION

Optical feedback interferometry (OFI) is a technique allowing the measurement of physical parameters such as those related to motion, refractive index and acoustic angle [1–3]. It uses a laser as the light emitter, the interferometer and the receiver. When a laser illuminates a distant moving object, a small portion of the scattered Doppler-shifted light enters back in the laser cavity and produces a perturbation in the fundamental operational regime of the laser. This modulated signal is monitored and processed to further obtain information on the target.

OFI, also known as self-mixing interferometry, has been extensively studied and applied in mechatronics [4], mostly for the measurement of vibrations [5], displacements [6], velocity [7], absolute distance of solid targets [8] and more recently for the study of propagation of sound waves [9]. However, its implementation in accurate fluid flow measurement systems is rather recent. For sensing in fluidic systems, OFI sensors have been implemented primarily as laser velocimeters, which have demonstrated experimentally

their capabilities to measure slow flows down to $26 \mu\text{m/s}$ [10]. In optical feedback flowmetry, the back-scattered light is generated by particles flowing in a fluid. As in Laser Doppler Velocimetry (LDV), the Doppler frequency shift is related to the particles velocity. Still, measuring velocity with accuracy is challenging and at the same time an increasing need for the biomedical, chemical and industrial communities.

OFI sensors are extremely attractive as they require minimal optical components. In addition, OFI uses a self-alignment scheme which avoids the complex arrangements required by other light based sensing techniques such as LDV and Optical Coherence Tomography (OCT), which perform properly in terms of spatial resolution and accuracy.

In this paper, we review the optical feedback phenomenon in semiconductor laser from basics to applications in the frame of fluid flow measurement. The article is structured as follows: First, we present a brief chronological evolution of the optical feedback interferometry. Further on, the fundamental principles of the optical feedback effect are presented for the case of fluid flow sensing. Then, the

equations describing the behavior of a laser subject to external feedback are presented and a model developed for the case of optical feedback flowmetry is derived. In addition, we present practical applications of OFI sensors as laser velocimeters applied to the detection of flowing particles in a microchannel, the analysis of unsteady flows and the *in-vivo* assessment of blood perfusion in skin.

II. HISTORY OF THE OPTICAL FEEDBACK PHENOMENON FOR SENSING PURPOSES

The history of optical feedback started almost immediately after the invention of the laser. In most cases optical feedback, or the mixing of the original and scattered electromagnetic waves in the laser cavity, was considered as a parasitic effect affecting both laser's frequency and amplitude. The first demonstration of the potential capabilities of the technique in sensing applications started in 1963 with the work of King and Steward [11]. Their articles demonstrated the feasibility of optical feedback to measure displacement even though as little as 0.1 % of scattered light from an object distant up to 10 m entered back inside the lasing cavity. In a clear attempt to extend the utility of the phenomenon of optical feedback in lasers in the general field of metrology, King and Steward filed a patent application in 1968 that introduced a general discussion on the potential of optical feedback interferometry for measuring physical parameters [12].

During the sixties, optical arrangements were designed and mounted in order to avoid the effect of external feedback entering back in the resonant cavity of the laser [13]. The first application in velocimetry was reported as early as 1968 when Rudd proposed the first Doppler velocimeter using the optical feedback effect in He-Ne gas laser [14].

Gas lasers were continuously used in the seventies. In 1972, Honeycutt and Otto reported the utilization of a CO₂ laser for range finding [15]. A few years later, a feedback-induced device was reportedly employed in reading a compact disc [16]. An OFI displacement sensor was proposed by Donati in 1978 using a combination of analog circuitry with an He-Ne laser [17].

It was in the eighties when OFI started to be employed in sensors incorporating semiconductor lasers, thanks to the advent of laser diodes. In 1980, Lang and Kobayashi [18] conducted a study on the phenomenon of external feedback in laser diodes and developed the equations ruling their behavior while subject to optical feedback effect. Later on, Shinohara used laser diodes for velocity measurements [19].

OFI's ability to measure velocity led to its implementation for sensing purposes in diverse fluidic applications. Koelink and de Mul proposed and demonstrated the first OFI based flowmeter in 1992 [20] [21]. The first optical feedback flow sensor accurately measured the flow velocity and these measurements were validated with a linear relationship obtained between the flow rate and the measured velocity. Since then, OFI sensors have been tested and implemented for flow assessment in fluidics, microfluidics and general flowmetry with interest in chemical and biomedical

engineering. Implementations include the measurement of blood flow over skin [22], the assessment of blood perfusion in tissue [23] [24] and drop measurements in clinical equipment [25]. Moreover, this technique is currently being actively employed for the study of shear-thinning and parallel flows in small channels [26] [27] as an alternative optofluidic sensing technique [28].

III. OPTICAL FEEDBACK FOR FLOW MEASUREMENTS

This section presents the basic principles of OFI applied to velocity measurements of flows. The main features of the interaction of the laser beam with the carrying scattering particles are posed and analyzed. Further on, the fundamental equations of the laser under external feedback are presented and a model is developed to determine the impact of multiple scatterers on the laser amplitude changes.

III.1. Particular features of laser-fluid interaction

The sensing mechanism of the optical feedback interferometry technique applied to flow measurements depends on the interaction of a laser beam and the particles embedded in the flow. There are particular features that models and approximations need to consider. The following aspects are distinctive:

- Light travels through a gradient of refractive indexes as it propagates across different materials until it reaches the particles in the flow.
- Many particles in the flow may be illuminated at once; hence the contribution to the optical feedback signal has a frequency signature characterized by a distribution of frequencies correlated to a plurality of particles traveling at different velocities.
- The illuminated volume where particles in the flow contribute to the optical feedback affecting the laser has three dimensional spatial components.
- Light scattered by small particles in a flow generate a diffusion pattern where the scattered electromagnetic field vectors are randomly distributed all over a round solid angle. This implies that the detection of light from fluidic systems interrogated by optical feedback interferometry is poor with respect to the sensing of solid targets.

It is important to take into consideration also that particles may behave different from the fluid so that they do not follow perfectly the flow hydrodynamics.

III.2. Theory of optical feedback applied to multiple scatterers

Two options are possible to describe the behavior of the laser diode under optical feedback: first, the three mirror cavity (the third mirror being the target) can be reduced to a two-mirror equivalent cavity from which the laser rate equations can be deduced [29]; second, the optical feedback can be seen as a perturbation of the established

lasing systems and, in this case, an additional term can directly be added to the field or photon rate equation that represents the contribution of the back-scattered light. This second approximation is known as the Lang and Kobayashi model [18]. A discussion on the advantages and the inconveniences of both modeling methods is presented in [30]. The conclusion of this study shows that, despite the equivalent cavity method is the most exact method, the Lang and Kobayashi perturbation approach is well suited for low feedback levels and quasi steady state analysis of the optical feedback phenomenon.

In the case where the optical feedback is provided by particles flowing in fluids, where the back-scattered power is described by the Mie theory, the feedback level remains very low. We have derived the Lang and Kobayashi method as originally proposed by Zakian [31] to demonstrate the contribution of multiple scatterers. For an equivalent analysis based on the compound cavity model, we refer the readers to a recent publication [32].

The modeling approach is based on the description of the established electric field propagating inside the laser cavity E that is subject to an external perturbation. It is represented by the the complex envelope of the electric field:

$$\frac{d}{dt}E(t)e^{j\omega t} = [j\omega_N + \frac{1}{2}\Gamma G(N - N_{tr})]E(t)e^{j\omega t} + F(t), \quad (1)$$

where ω is the laser mode angular frequency, ω_N is the cavity mode angular frequency ($\omega_N = \pi kc/n_c L_c$, with k an integer, L_c the laser cavity length and n_c the refractive index), Γ stands for the laser mode confinement factor, N is the carrier density, N_{tr} is the carrier density at transparency, G is the stimulated emission gain and $F(t)$ is the feedback induced perturbation term.

Depending on the nature of the target, $F(t)$ can adopt different formulations:

- In the case of a unique and fixed target located at a distance L_{ext} from the laser cavity,

$$F(t) = \tilde{\kappa}E(t - \tau)e^{j\omega(t-\tau)}, \quad (2)$$

where τ is the external cavity roundtrip time of flight ($\tau = 2n_{ext}L_{ext}/c$) and $\tilde{\kappa}$ is the feedback coupling coefficient defined as:

$$\tilde{\kappa} = \frac{\kappa}{\tau_c} = \frac{1}{\tau_c}(1 - r_2^2)\frac{r_{ext}}{r_2}. \quad (3)$$

Here, κ is the coupling strength of the laser with the external cavity, τ_c is the laser cavity roundtrip time of flight ($\tau_c = 2n_c L_c/c$), r_2 the reflectivity of the laser front mirror and r_{ext} the ratio of the back-scattered power actually re-entering the laser cavity over the emitted power.

- In the case of a unique target in translation that induces a Doppler shift:

$$f_D = \frac{\omega_D}{2\pi} = \frac{2V\omega}{2\pi(c + V)}, \quad (4)$$

is dependent on the target's velocity projection on the optical axis V and the feedback contribution becomes

$$F(t) = \frac{\kappa}{\tau_c}E(t - \tau)e^{j(\omega + \omega_D)(t-\tau)}. \quad (5)$$

- In the case of multiple targets, each one scatters back toward the laser cavity its own contribution so that:

$$F(t) = \sum_i F_i(t), \quad (6)$$

with each F_i that can be written as:

$$F_i(t) = \frac{\kappa_i}{\tau_c}E(t - \tau_i)e^{j(\omega + \omega_{D,i})(t-\tau_i)}, \quad (7)$$

that takes into account the fact that each particle is located at a specific distance from the target which induces a particular time of flight τ_i , and that the reflectivity of each particle has its proper characteristics so that

$$\kappa_i = (1 - r_2^2)\frac{r_{ext,i}}{r_2}, \quad (8)$$

and that each particle has its proper velocity projection along the optical axis inducing

$$\omega_{D,i} = \omega \frac{2V_i}{c + V_i}. \quad (9)$$

Thus, considering equation (1) with the perturbation $F(t)$ described as (7) obtaining the variation of the laser output power induced by the particle optical feedback consists in solving the set of rate equations for the laser. We obtain this set of equations by separating the real and the imaginary part of the field equation, considering that the phase of the electric field $\phi(t) = \arctan \frac{\Im(E(t))}{\Re(E(t))}$ and introducing the carrier density equation. Since the Doppler shift induced by the particle velocity occurs at very low frequency when compared to the laser optical frequency, the usual approximation of the quasi-steady state regime can be done: $E(t - \tau) \sim E(t)$, therefore:

$$\frac{dE(t)}{dt} = \frac{1}{2}\Gamma G(N - N_{tr})E(t) + \sum_i \frac{\kappa_i}{\tau_c}E(t) \cos(\omega_{D,i}t + \phi_i), \quad (10)$$

$$\frac{d\phi(t)}{dt} = \frac{1}{2}\alpha\Gamma G(N - N_{tr}) + \sum_i \frac{\kappa_i}{\tau_c} \sin(\omega_{D,i}t + \phi_i), \quad (11)$$

$$\frac{dN(t)}{dt} = \frac{1}{qV_a} - G(N - N_{tr})S - \frac{N}{\tau_n}, \quad (12)$$

where α is the linewidth enhancement factor, ϕ is the phase term of the electric field E , ϕ_i is a random phase, q is the elementary charge, V_a is the laser active volume, τ_n is the carrier lifetime and S is the photon density which is linked to the field amplitude by:

$$S \propto E \cdot E^*, \quad (13)$$

which allows to re-write (10) as

$$\frac{dS(t)}{dt} = G(N - N_{th})S(t) - \frac{S(t)}{\tau_S} + \sum_i \frac{\kappa_i}{\tau_c}S(t) \cos(\omega_{D,i}t + \phi_i). \quad (14)$$

In (14), τ_s is the photon lifetime and N_{th} is the carrier density at threshold. Solving the set of equations (10)-(14) in the case of the quasi-steady state regime has been exposed in many ways [1] [30]. Following the same methodology leads to write the following equations for phase and amplitude respectively:

$$\omega_F - \omega_0 = \alpha \sum_i \frac{\kappa_i}{\tau_C} \cos(\omega_{D,i}t + \phi_i) + \sum_i \frac{\kappa_i}{\tau_C} \sin(\omega_{D,i}t + \phi_i), \quad (15)$$

$$S_F = S_0 \left[1 + 2 \frac{\tau_S}{\tau_C} \sum_i \kappa_i \cos(\omega_{D,i}t + \phi_i) \right], \quad (16)$$

where ω_F and ω_0 are the laser angular frequency with and without feedback respectively and S_F and S_0 are the photon densities under similar hypothesis. Equation (15) can be simplified in

$$\omega_F - \omega_0 = \sqrt{1 + \alpha^2} \sum_i \frac{\kappa_i}{\tau_C} \sin(\omega_{D,i}t + \phi_i + \arctan \alpha), \quad (17)$$

while (16) directly provides a simple and easy relationship for the laser emitted power variations that are proportional to the photon density

$$P_F = P_0 \left[1 + \sum_i m_i \cos(\omega_{D,i}t + \phi_i) \right], \quad (18)$$

where m_i represents the modulation indexes relative to the i^{th} particle and is given by:

$$m_i = 2 \frac{\tau_S}{\tau_C} \kappa_i. \quad (19)$$

It shall be noted that despite the Doppler shift $\omega_{D,i}$ is a function of ω_F , in the case of optical feedback in fluids where the low back-scattered power requires a short range of operation (usually tens of millimeters), the changes in laser frequency can be neglected for the calculation of the optical power variations.

To validate the model, the equation (18) has been implemented in MatlabTM for a 1D - distribution of velocities along the optical axis that follows Poiseuille's law for the velocity distribution in a circular duct [33]. The parameters used in the modeling for the laser and the target are: Electric field angular frequency $\omega=2.4 \cdot 10^{15}$ rad/s at $\lambda=785$ nm; Refractive index in the laser cavity $n_C=3.5$; Laser cavity length $L_C=3 \cdot 10^{-4}$ m; External cavity length $L_{ext}=0.1$ m; Reflexion coefficient of the front mirror of the laser $r_2=5\%$; Photon lifetime $\tau_s=10^{-9}$ s. The flow parameters are as follows: the maximum velocity in the $320 \mu\text{m}$ diameter channel is 0.2 m/s, the flow direction makes an angle of 80° with the optical axis. Figure 1 shows the analytical velocity profile. The light absorption in the fluid has been fixed so that the penetration depth is 1 mm. A random phase ϕ_i has been given for each position as originally proposed by Nikolić et al. [34], which takes into account both the phase shift induced by the time of flight in the external cavity and the random phase shift induced by the scattering effect on the particle. Also, for the

sake of understanding the signal spectrum, a white Gaussian noise has been added to the signal through Matlab's rand function.

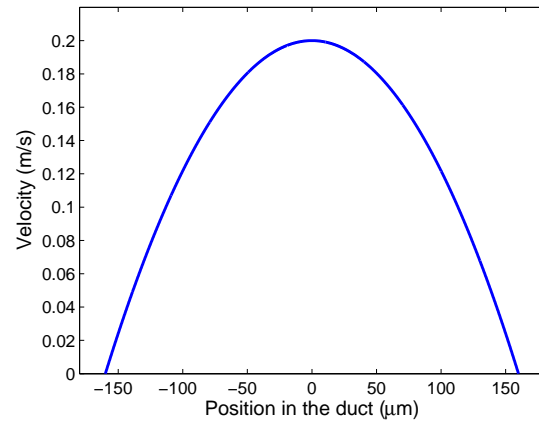


Figure 1. Velocity distribution along the optical axis in the duct. The maximum velocity in the center of the duct is 0.2 m/s and the distribution corresponds to a Poiseuille laminar flow following a parabolic velocity profile. The center of the duct is represented in position $x = 0$.

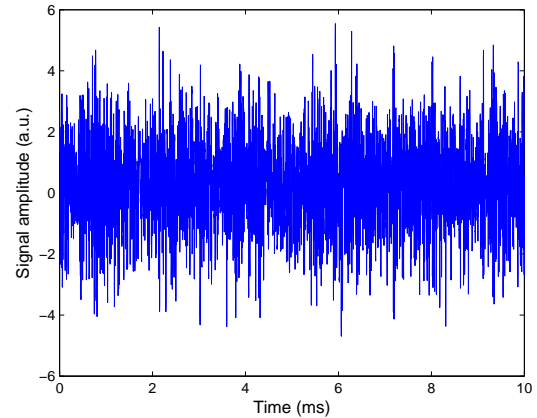


Figure 2. Time domain representation of the OFI signal corresponding to a flow moving inside a $320 \mu\text{m}$ diameter channel at 0.2 m/s.

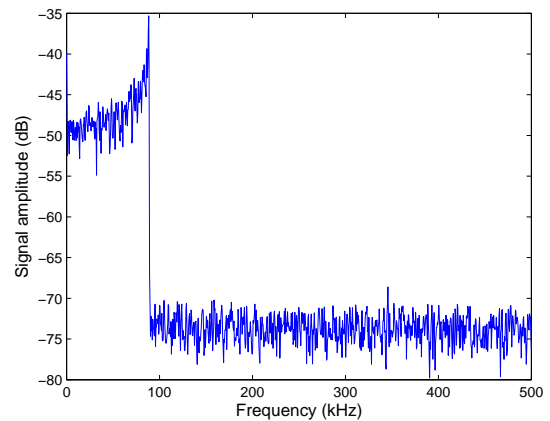


Figure 3. Frequency domain representation of the OFI signal shown in Fig. 2. The fundamental frequency at 88.4 kHz corresponds to the maximum velocity of a flow moving in the center of the channel at 0.2 m/s.

The time domain signal presented in Fig. 2 is clearly not deterministic and the unique manner to obtain the information on the velocity of the fluid is the spectral

analysis. The maximum velocity considering the incident angle and the laser wavelength is expected to produce a Doppler shift of 88.4 kHz, which corresponds roughly to the maximum frequency observed in the distributed spectrum of Fig. 3.

IV. PRACTICAL APPLICATION OF OFI SENSORS: VELOCIMETRY

In OFI based velocimetry (flowmetry), the Doppler spectrum is analyzed to obtain the information regarding the velocity of moving object (particles). The fundamental frequency observed in the power spectral density is directly correlated to the target's velocity. For low concentrated fluids, i.e fluids with few percentage of scattering centers guaranteeing the single scattering regime, the maximum velocity of the flow can be calculated using a simple expression given by:

$$v = \frac{\lambda f_D}{2n \cos \theta} \quad (20)$$

where λ is the laser wavelength, f_D is the Doppler frequency generated by particles, n is the refractive index of the surrounding medium and θ is the angle between the laser axis and the particle direction.

This means that the refractive index of the fluid and the angle between the laser and the velocity vector of the flow need to be known. By controlling these simple parameters, the velocity can be measured non-invasively with resolutions comparable to LVD and OCT systems.

However, the processing of the signal leading to a quantitative measurement of the flow is strongly dependent on the concentration of scatterers in the flow. As a consequence, the spectrum morphology is affected by the multiple scattering leading to multiple Doppler shifts before the photons enter back in the laser cavity. This issue is complicated to address, but from a theory developed by Bonner in 1980 [35], the fundamental frequency can be determined by using the center of gravity of a frequency distribution. The desired frequency is thus determined using the following formulation:

$$f_{ave} = \frac{\int_0^{\infty} f \cdot p(f)}{\int_0^{\infty} p(f)}, \quad (21)$$

where f_{ave} is described by as the average Doppler frequency equal to the ratio of the first order moment (M^1) and the zero order moment (M^0). M^1 is proportional to the average velocity times the number of particles generating Doppler shifts and M^0 is related to both the number of particles generating Doppler shifts as well as to the Doppler shift values [21] [23] [36]. $p(f)$ is the OFI power spectrum obtained as the square module of the Fast Fourier Transform of the signal.

It should be noted that from the average frequency calculated from expression (21) the maximum velocity of the flow

cannot be directly obtained. So, the geometry of the duct should be known to calculate the velocity distribution. For a duct with circular cross-section, $f_D = 2f_{ave}$. In a square cross-section channel, the ratio of the velocities (and corresponding frequencies) is 2.09. For cross-sections with particular geometries, such as rectangular, the relation of the corresponding velocities will depend on the aspect ratio [37].

V. GENERAL OFI ARCHITECTURE

Depending on specific applications, OFI sensors may incorporate different optical components. In some cases, the laser beam spot needs to be very small. This is typical of the measurements realized in microfluidic channels. For example, there are reports of OFI flowmeters based on a dual-lens configuration [26] [27] [38], single lens configuration [22] or lens-free architectures [39]. Here we present a single lens OFI velocimeter that was used in our experiments.

A simplified representation of the system is depicted in Fig. 4. The laser diode is coupled to a lens that focuses the coherent radiation on the target. The assembly is tilted certain angle θ that is generally fixed to obtain the best signal to noise ratio in the OFI signal. The power variations of the laser can be measured directly from the changes in the junction voltage. However, many semiconductor lasers integrate a photodiode in the laser module. In such a case, the detected photo-current is used and amplified by a custom built transimpedance amplifier. In our experiments described further in the text, we have used the amplification of the signal from the photodiode, which is then registered by a data acquisition card.

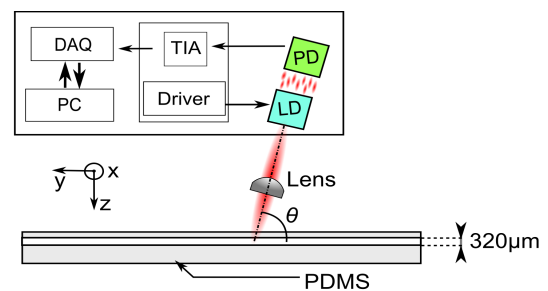


Figure 4. Schematic representation of the OFI sensing system. LD - Laser diode, PD- Photodiode, DRIVER- Laser driving electronics, TIA- Transimpedance amplifier, DAQ- Data acquisition card, PC- Personal computer. The target is here represented by a PDMS-made microfluidic channel in which flow direction is y.

VI. SENSING APPLICATION: PARTICLE DETECTION AND LOCATION

Particle detection in fluids has been subject of great interest in current applications in fluid dynamics and transport phenomena [40]. In this section, we demonstrate the capabilities of the optical feedback interferometry (OFI) sensing technique combined with a proper signal processing for online particle detection in microfluidic devices. The

detection of single suspended particles in a microchannel is a direct application of OFI sensing systems in the single scattering regime produced by the interaction of a laser beam with individual particles acting as scattering centers.

There are previous attempts to use OFI for particle tracking and size estimation [31] [41], but to the best of our knowledge, none of the proposed systems has accomplished an online measurement architecture applied to quality control of fluid flows present in industrial processes or laboratory environments.

We propose in what follows using the OFI signal in a semiconductor laser to characterize flowing particles in a microchannel. The objective behind the proposed methodology is the development of a new optical tool for quality control in chemical, pharmaceutical and biomedical engineering that can be implemented for online inspection of fluids that should supposedly be free of particles. The perturbation of the laser signal is used to trigger an online processing allowing the characterization of a particle flowing across the illuminated volume.

VI.1. Microfluidic channel

The cylindrical polydimethylsiloxane (PDMS) fluidic chip consists of a unique circular-cross section channel with internal diameter of $320\ \mu\text{m}$. The PDMS chip was made of silicon elastomer (Sylgard 184) which is mixed with a curing agent mixed at a 10:1 ratio, cured at ambient temperature and cooled for 24 hours. To manufacture the channel inside the PDMS, a $320\ \mu\text{m}$ diameter optical fiber was inserted inside the silicon elastomer before curing and pulled out once the mixture cured completely, thus forming a cylindrical duct inside the PDMS.

VI.2. OFI sensor, signal detection and processing

The OFI sensor uses a single lens configuration as depicted in Fig. 4. The laser diode (Thorlabs L785P090, emitting at 785 nm, optical power is 90 mW) is located at twice the focal distance of the focusing lens (Thorlabs C240TME-B, focal length $f = 8\ \text{mm}$). The lens is positioned at distance $2f$ from the microchannel and focused exactly in the middle of the cylindrical duct. The assembly is tilted 80° with respect to the flow direction. The signals of the integrated photodiode with 4096 points were sampled at 500 kHz and acquired using a BNC-2110 National Instruments data acquisition card.

The detection mechanism is described as follows. Light emitted by the laser beam traverses a cylindrical transparent microchannel where a flow of water seeded with some particles is pumped at a constant flow rate. The particles scatter the incident light as they cross the illuminated volume. A small portion of the scattered waves enters in the laser and produces a burst in intensity that is detected by the photodiode.

A typical signal showing the perturbation in the laser due to the optical feedback produced by flowing particles is

presented in Fig. 5. The signal is characterized by a stable amplitude, and the burst with amplitude and frequency modulation corresponds to the interval when a particle interacts with the light.

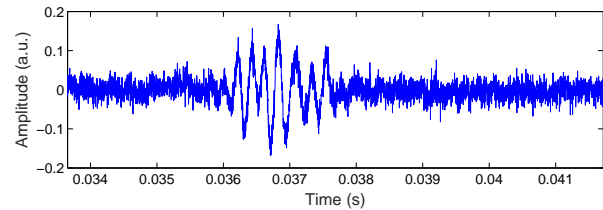


Figure 5. Optical feedback signal showing the characteristic signal and the burst produced by a particle as it passes through the illuminated volume. Peak to peak threshold was 0.2.

The detection mechanism comprises an automated system capable of detecting the difference of amplitude from peak to peak that is higher than a pre-defined threshold adequately selected from the inspection of the raw signal without particles. A custom made LabVIEW™ software was programmed to automatically trigger an instruction and display in the computer screen the signal with the burst. Then, the interval containing the burst is adequately chosen to apply the signal processing.

The signal burst shows a modulation of the laser where interferometric fringes can be easily identified. These fringes contain the information on the particle's kinematic features. A Hilbert Transform (HT) is performed in the smoothed burst interval and the unwrapped phase is normalized and plotted. Thereby, fringes are confirmed by a well-established fringe detection algorithm [42]. The outcome of the processing is depicted in Fig. 6. Fully developed fringes are used to determine the burst interval, represented in between the square points. Depending on the particle size and their position in the channel, the burst time will be longer or shorter in correspondence to their velocity.

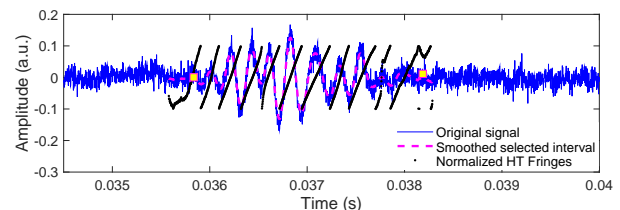


Figure 6. Signal processed to confirm fringes in the burst. White squares indicate the selected beginning and the end of the burst. The Hilbert Transform representation is normalized by $10\ \pi$ to fit the size of the amplitude.

The characteristic frequency of the selected interval is calculated from the power spectral density (PSD) of the autocorrelation of the portion of the signal containing the burst. Figure 7 shows the power spectrums corresponding to the segment of the burst depicted in Fig. 6 and to its autocorrelation. Using the frequency corresponding to the maximum in the spectrum, selected either from the Fast Fourier Transform (FFT) of the raw burst or from its autocorrelation, the velocity of the particle can be easily determined using the expression (20). The convenience of

calculating the PSD from the autocorrelation lies on the fact that it allows the amplification of the power spectrum, which is useful in those cases where very low scattered light enters in the laser.

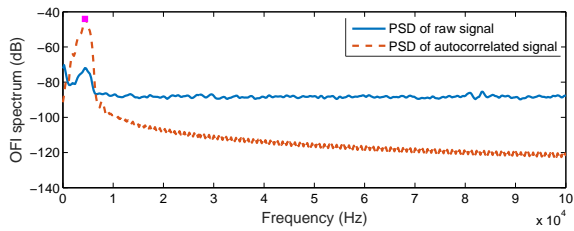


Figure 7. Signal spectrum calculated from the fast Fourier transform and from the autocorrelation of the signal. Both maximums hold the same Doppler frequency. The square is used to represent the frequency of the maximum correlated to the velocity of particles flowing inside the PDMS channel.

VI.3. Particle detection and location experiment

The optical feedback system was tested with the microparticles and the full methodology was applied using an online system customized in LabVIEW™. Three different spherical microparticles are used in this experimental work: iM30K and S22 glass particles from 3M™ and polystyrene particles PS-R-4.9 from Microparticles GmbH. A solution containing 100 mL of demineralized water is prepared and 0.001 % of particles of each kind (determined by mass) are merged in the water. Every dilution is prepared with one type of particles at the time. A flow-controlled syringe pump (Harvard Apparatus Pico 11 Plus) is used to introduce the seeded flow in the channel at 20 $\mu\text{L}/\text{min}$. For this flow rate, the analytical flow profile can be easily determined with the simple equation of Poiseuille flows given by:

$$v(r) = v_{max} \left(1 - \left[\frac{r}{R} \right]^2 \right), \quad (22)$$

where $R = 160 \mu\text{m}$ is the radius of the circular cross section of the flowchannel, r is the distance from the wall to the center of the cylinder and v_{max} is the velocity in the center of the channel. In the case of ducts with circular cross sections, $v_{max} = 2Q/A$ where Q is the volumetric flow rate and A is the cross section surface.

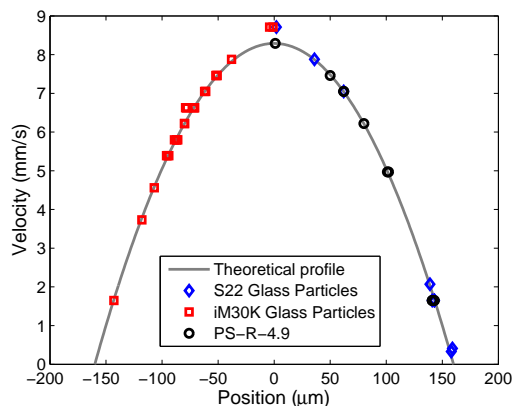


Figure 8. Particles location inside the microchannel. Positions are given with respect to the center of the channel. The theoretical profile is calculated from equation 22.

Figure 8 shows the measurements performed with different microparticles during 10 minutes. The flowing particles are located in terms of distance with respect to the center of the channel. It should be noted that the method presented here enables the particle location, but does not provide an efficient way to discriminate if the particles passed above or below the channel center.

As evidenced by these results, the developed methodology enables the location of flowing particles in microfluidic devices, thus opening potential applications of optical feedback interferometry in the analysis of fluidic systems at the microscale for control and monitoring systems. The analysis presented here, may be extended to biological fluids where cells could be interrogated in small vessels.

VII. SENSING APPLICATION: NON-STEADY FLOW VELOCITY MEASUREMENT

Another application where OFI sensors can perform valuable and useful measurements is the analysis of unsteady flows. This is particularly interesting for biomedical and chemical fields where fluids are subject to periodic forcing. One of the examples is the heart beat in arteries. In most cases, the local velocity of the flow is a major interest. For the case of multiple scattering, the weighted moment presented earlier in the main text provides the quantitative information of the average frequency to further determine the average velocity of a particular flow.

VII.1. Unsteady flow assessment

The infrared laser OFI sensor described in the previous section was tested to analyze unsteady flows in a millifluidic configuration. The system is presented in Fig. 9.

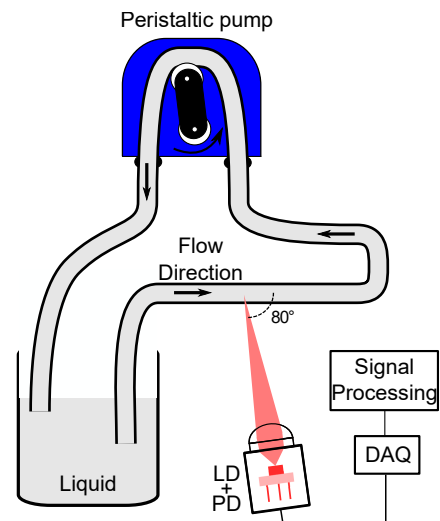


Figure 9. OFI system for non-steady flow velocity measurement. LD- Laser Diode, PD- Photo-diode, DAQ- Data Acquisition Card; Liquid is full-cream milk diluted in water at 79.75 %.

Note that the flow direction is intentionally drawn as going towards the laser. This scheme does not affect the OFI

measurement. The sensor is again tilted 80° with respect to the cylindrical transparent tube. We interrogate continuously the flow of a two-pressing-members peristaltic pump (Seko PR1) and reconstruct the periodicity of the pumped fluid. A solution of full-cream milk diluted in water at 79.75% is used in this experiment. The pump was chosen so that its technical features are unknown, and the flow rate is externally driven by a potentiometer without controlling quantitatively the pumping rate. Signals were sampled at 500 kHz and each contains 4096 points averaged over ten consecutive measurements. The experimental data is registered in a computer with a National Instruments Data Acquisition Card (USB-6361).

Figures 10 to 12 show the reconstructed measured flow during 30 s for three arbitrary positions of the pump's potentiometer. As can be easily appreciated, the continuous processing of the OFI signal enables the direct measurement of the non-steady flow and the reconstruction of its periodicity in time. This is especially important in those cases where the fluid flows in close liquid-filled circuits. In such circuits, once the tube is filled there is no way to know from simple observation if the fluid is moving or not, thus an interrogation with a non-destructive method is necessary.

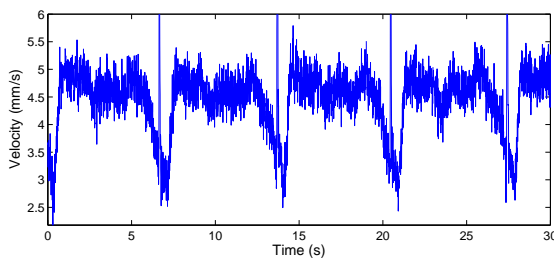


Figure 10. Unsteady flow velocity measured during 30 seconds. Position of the potentiometer is 1.

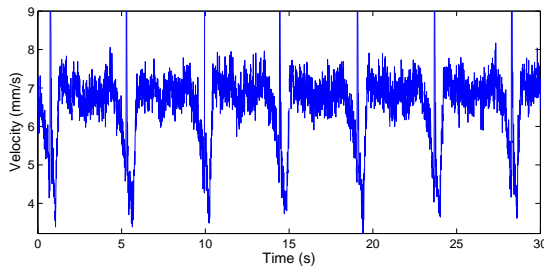


Figure 11. Unsteady flow velocity measured during 30 seconds. Position of the potentiometer is 4.

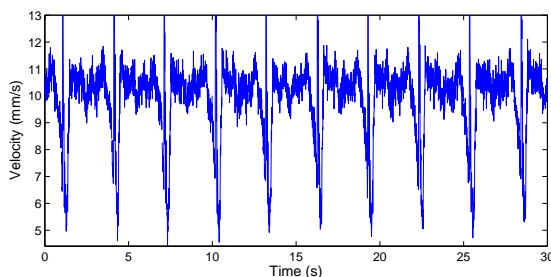


Figure 12. Unsteady flow velocity measured during 30 seconds. Position of the potentiometer is 7.

The results presented in Figures 10 to 12 demonstrate that optical feedback interferometry sensors may be well-suited to interrogate flows in biomedical scenarios, being the measurement of heart beat in arteries a potential implementation. Other fields related to rheology and transport phenomena in chemical engineering may find benefit as well.

VIII. SENSING APPLICATION: BLOOD PERFUSION ASSESSMENT

One of the fields related to biomedical studies that may find a powerful tool in optical feedback interferometry sensors is the microvascular research. Indeed, OFI systems could be utilized in the analysis of perfusion in skin to generate quantitative information related to malignant tissue or microcirculation associated to tissue irrigation.

The analysis of this new environment requires to adapt the processing to this particular situation. Blood flow in skin is not necessarily straight and therefore the velocity vector necessary to correlate the detected frequency to the velocity is unknown. However, using the moment zero present in the denominator of equation (21) provides a parametric quantification of the flow. We present in this section a demonstrative *in-vivo* experiment for quantifying the perfusion in skin using the OFI signal.

VIII.1. *In-vivo* experiment in skin

The experiment consist on coupling an optical feedback interferometry sensor to a scanning system and calculating the zero moment for every position in the scan. Since the calculation of the moment zero is an integration of the spectrum, the outcome of the processing will indicate a different value for a scanned zone with microcirculation associated with respect to a zone with non-biological material. To this end, we scanned a portion of a finger passing through a plastic tape. Figure 13 presents the real set-up conditions, where the finger is pointed with the OFI sensor and the laser scans 100 points along 10 mm in the vertical direction, thus passing from a zone with perfusion flow to the taped zone and then to a new portion of the skin. The quantifier parameter moment zero is expected to decrease in the zone occupied by the tape as it does not contribute to the OFI signal due to the absence of scattering centers.

The OFI sensor used in this experiment is composed of a semiconductor laser (Hitachi HL7451G) emitting at 785 nm and driven by an injection current of 100 mA which is coupled to a plano-convex lens (Thorlabs LA1951-B, focal length $f = 25.4$ mm). The sensor is tilted 70° with respect to the target. A National Instruments BNC-2110 data acquisition card is used to record OFI signals containing 8192 points, sampled at 500 kHz and every recorded data corresponds to ten continuously averaged power spectral densities of the raw signals.

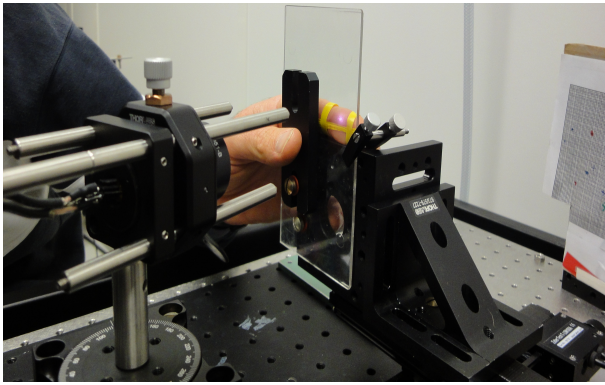


Figure 13. Optical feedback interferometry sensor coupled to a scanning system for quantifying the perfusion flow in skin. The plastic tape is added to scan a zone without microcirculation associated.

The results of the scan are presented in Fig. 14. The area covered by the tape is represented by an arrow. The scanned line indicates that the OFI signal is higher in the zone where the laser points directly to the skin and it decreases when it enters in contact with a zone without scattering centers. OFI sensing in skin can be performed to interrogate blood perfusion within a few mm deep in the skin. However, the sensor should be adequately adapted according to specific purposes and the laser and optical parameters should be carefully optimized in terms of optical power and light collection with the lens to guarantee an efficient measurement with an OFI architecture.

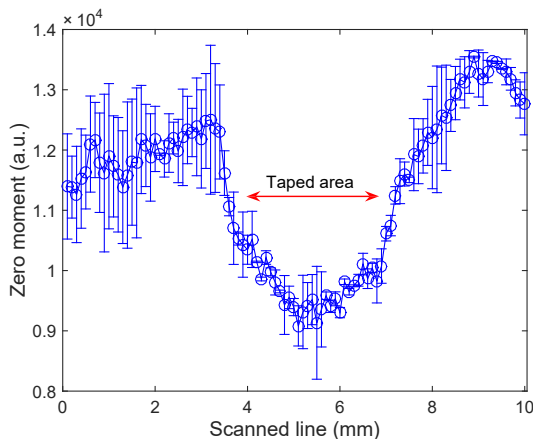


Figure 14. Zero moment calculated from the OFI signal for a scanned line in the finger, where the laser passes from the skin to the plastic tape. Open circles indicate the mean value averaged over 4 consecutive scans and the errorbars indicate the standard deviation associated to these scans.

OFI based sensing provides then an alternative way to measure perfusion in skin, thus its implementation in medical procedures is direct and suitable. The methodology presented here may be well-suited for microvascular research. Other potential applications can be assimilated for the study of wounds, scars and keloids.

IX. CONCLUSIONS

We presented the fundamentals of the Optical Feedback Interferometry sensing technique in the frame of flowmetry.

A model derived from the theoretical approximation based upon the Lang and Kobayashi rate equations is presented and tested in a flow inside a microfluidic channel. We presented some potential applications of this technique in fluidic systems that may find relevance in chemical and biomedical engineering.

ACKNOWLEDGMENTS

This work was supported by the French Embassy in Havana that partially funded the PhD studies of the first author in Toulouse, France.

REFERENCES

- [1] T. Taimre, M. Nikolić, K. Bertling, Y. L. Lim, T. Bosch and A. D. Rakić. *Adv. Opt. Photon.* 7, 570 (2015).
- [2] J. Perchoux, A. Quotb, R. Atashkhoei, F. J. Azcona, E. E. Ramírez-Miquet, O. Bernal, A. Jha, A. Luna-Arriaga, C. Yanez, J. Caum, T. Bosch and S. Royo. *Sensors* 16, 694 (2016).
- [3] J. Li, H. Niu and Y. Niu. *Opt. Eng.* 56, 050901 (2017).
- [4] S. Ottonelli, M. Dabbicco, F. De Lucia, M. di Vietro and G. Scamarcio. *Sensors* 9, 3527 (2009).
- [5] U. Zabit, R. Atashkhoei, T. Bosch, S. Royo, F. Bony and A. D. Rakić. *Opt. Lett.* 35, 1278 (2010).
- [6] C. Bes, G. Plantier and T. Bosch. *IEEE Trans. Instrum. Meas.* 55, 1101 (2006).
- [7] L. Scalise, Y. Yu, G. Giuliani, G. Plantier and T. Bosch. *IEEE Trans. Instrum. Meas.* 53, 223 (2004).
- [8] F. Gouaux, N. Servagent and T. Bosch. *Appl. Opt.* 37, 6684 (1998).
- [9] K. Bertling, J. Perchoux, T. Taimre, R. Malkin, D. Robert, A. D. Rakić and T. Bosch. *Opt. Express* 22, 30346 (2014).
- [10] R. Kliese, Y. L. Lim, T. Bosch and A. D. Rakić. *Opt. Lett.* 35, 814 (2010).
- [11] P. G. R. King and G. J. Steward. *New Sci.* 17, 180 (1963).
- [12] P. G. R. King and G. J. Steward (1968). U.S. Patent 3409370.
- [13] N. , G. Mourat, F. Gouaux and T. Bosch. *Proc. of SPIE* 3479, 76-83 (1998).
- [14] M. Rudd. *J. Sci. Instrum.* 1, 723 (1968).
- [15] T. E. Honeycutt and W. Otto. *IEEE J. Quantum Electron.* 8, 91-92 (1972).
- [16] A. Seko, Y. Mitsuhashi, T. Morikawa, J. Shimada and K. Sakurai. *Appl. Phys. Lett.* 27, 140 (1975).
- [17] S. Donati, *J. Appl. Phys.* 49, 495 (1978).
- [18] R. Lang and K. Kobayashi. *IEEE J. Quantum Electron.* QE-16, 347 (1980).
- [19] S. Shinohara, A. Mochizuki, H. Yoshida and M. Sumi. *Appl. Opt.* 25, 1417 (1986).
- [20] M. H. Koelink, M. Slot, F. F. M. de Mul, J. Greve, R. Graaff, A. C. M. Dassel and J.G. Aarnoudse. *Appl. Opt.* 31, 3401 (1992).
- [21] F. F. M. de Mul, M. H. Koelink, A. L. Weijers, J. Greve, J. G. Aarnoudse, R. Graaff and A. C. M. Dassel. *Appl. Opt.* 31, 5844 (1992).

- [22] S. K. Özdemir, I. Ohno and S. Shinohara. *IEEE Trans. Instrum. Meas.* 57, 355 (2008).
- [23] F. F. M. de Mul, M. H. Koelink, A. L. Weijers, J. Greve, J.G. Aarnoudse, R. Graaff and A. C. M.Dassel. *IEEE Trans. Biomed. Eng.* 40, 208 (1993).
- [24] E. Figueiras, R. Oliveira, C. F. Lourenço, R. Campos, A. Humeau-Heurtier, R. M. Barbosa, J. Laranjinha, L. F. R. Ferreira and F. F. M. de Mul. *Med. Biol. Eng. Comput.* 51, 103 (2013).
- [25] M. Norgia, A. Magnani, D. Melchionni and A. Pesatori. *IEEE Trans. Instrum. Meas.* 64, 2113 (2015).
- [26] L. Campagnolo, M. Nikolić, J. Perchoux, Y. L. Lim, K. Bertling, K. Loubière, L. Prat, A. D. Rakić, T. Bosch. *Microfluid. Nanofluid.* 14, 113 (2013).
- [27] E. E. Ramírez-Miquet, J. Perchoux, K. Loubière, C. Tronche, L. Prat and O. Sotolongo-Costa. *Sensors* 16, 1233 (2016).
- [28] M. Nikolić, E. Hicks, Y. L. Lim, K. Bertling and A. D. Rakić. *Appl. Opt.* 52, 8128 (2013).
- [29] K. Petermann, *Laser diode modulation and noise.* (Kluwer Academic Publishers, Tokyo, 1991).
- [30] D. M. Kane and K. A. Shore. *Unlocking Dynamical Diversity: Optical feedback effects on semiconductor lasers* (John Wiley & Sons Ltd, Chichester, 2005).
- [31] C. Zakian, M. Dickinson and T. King, *J. Opt. A: Pure Appl. Opt.* 7, S445 (2005).
- [32] Y. Zhao, J. Perchoux, L. Campagnolo, T. Camps, R. Atashkhoeei and V. Bardinal. *Opt. Express* 24, 23849 (2016).
- [33] C. Riva, B. Ross and G. B. Benedek. *Invest. Ophthalmol. Vis. Sci.* 11, 936 (1972).
- [34] M. Nikolić, T. Taimre, J. R. Tucker, Y. L. Lim, K. Bertling and A. D. Rakić. *Electron. Lett.* 50, 1380 (2014).
- [35] R. Bonner and R. Nossal. *Appl. Opt.* 20, 2097 (1981).
- [36] M. Norgia, A. Pesatori and L. Rovati. *IEEE Trans. Instrum. Meas.* 59, 1233 (2010).
- [37] E. P. Pérez, L. R. Carrocci, J. A. de Carvalho Jr. and J. M. Neto. In *Crescendo. Ingeniería.* 3, 52 (2016).
- [38] M. Norgia, A. Pesatori and L. Rovati. *IEEE Sensors J.* 12, 552 (2012).
- [39] M. Norgia, A. Pesatori and S. Donati. *IEEE Trans. Instrum. Meas.* 65, 1478 (2016).
- [40] C. G. Ebeling, A. Meiri, J. Matineau, Z. Zalevsky, J. M. Gerton and R. Menon. *Nanoscale* 7, 10430 (2015).
- [41] S. Sudo, Y. Miyasaka, K. Nemoto, K. Kamikariya and K. Otsuka. *Opt. Express* 15, 8135 (2007).
- [42] A. L. Arriaga, F. Bony and T. Bosch. *App. Opt.* 53, 6954 (2014).